

Vitamin E Assisting Polymer Electrolyte Fuel Cells

Yingfang Yao^{1,2,3}, Jianguo Liu^{1,2,}, Wenming Liu^{1,3}, Ming Zhao¹, Bingbing Wu¹, Jun Gu^{1,2}, Zhigang Zou^{1,2,3,*}*

*¹Eco-materials and Renewable Energy Research Center, Department of Materials Science and Engineering,
National Laboratory of Solid State Microstructures, Nanjing University, 22 Hankou Road, Nanjing 210093,
China*

²Kunshan Innovation Institute of Nanjing University, Nanjing 210093, China

³Department of Physics, Nanjing University, 22 Hankou Road, Nanjing 210093, China

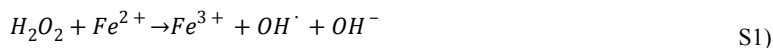
**Corresponding author. Tel.: +86 25 83621219; fax: +86 25 83686632. Email: jianguoliu@nju.edu.cn*

**Corresponding author. Tel.: +86 25 83686630; fax: +86 25 83686632. Email: zgzou@nju.edu.cn*

Materials and Methods

Ex situ chromogenic experiment

The sensitivity of Rhodamine B, Nafion, and α -TOH towards free radical reactive oxygen species (ROS) was evaluated by performing *ex situ* chromogenic experiments in a flask. 0.5 mM Fenton's catalyst, transition metal ions, i.e., Fe^{2+} , was added into 12.5 μ M rhodamine B aqueous solution. Certain amount of H_2SO_4 and α -TOH were then added into 50mL such solution, and ultrasonically oscillated until milk like solution was made. A known amount of H_2O_2 was then added to the flask and the drop in color fading was observed, recorded as the UV-vis light absorbance intensity decreased. This step was repeated several times, and after each addition of H_2O_2 , the absorbance intensity dropped. H_2O_2 decomposed into hydroxyl and hydroperoxyl radicals via the simplified Fenton's reaction shown below:



The observed color fading was due to the oxidation of the dye molecules by the hydroxyl and hydroperoxyl radicals generated during the reaction.

H_2SO_4 was then replaced with 0.4 g/L Nafion aqueous solution to evaluate the sensitivity of Nafion compared with rhodamine B and α -TOH. It was observed the inhibition of isopropanol to the Fenton agents (Fig. S3b). As a result, original commercial Nafion solution was thoroughly dried with the temperature of 60 $^{\circ}C$, followed with dissolution in deionized water to make a 10 wt% Nafion aqueous solution.

All the samples with certain concentration were prepared with 3 batches, and the detection of the absorbance intensity of each batch was repeated 3 times. And each spectra datum was then averagely recorded.

Preparation of regular and bilayer membrane electrode assembly (MEA)

50g 5 wt% Nafion/isopropanol solution was added into 22.5 g refluxed dimethyl sulfoxide (DMSO). The 10 wt% Nafion/DMSO solution was made with subsequent vacuum distillation to remove isopropanol in the solution. Then 0, 2.5, 5, 15 mg α -TOH were dissolved in 5 g such solution to make Nafion/0, 0.5, 1, 3 wt% α -TOH composite solution respectively. The composite solutions were then casted on a flat, balancing platform with the area of $8 \times 8 \text{ cm}^2$, heated with the temperature of 70 $^{\circ}C$ under air for 12 hours for solvent evaporation, and followed with 135 $^{\circ}C$ under N_2 for 1 hours for Nafion membrane curing. The composite membranes were then made with the average thickness at around 40 μ m. The made composite membrane appeared transparently yellow as the color of α -TOH, showing the successful addition of the antioxidant.

Cathode side testing membranes used in the *in situ* electrochemical detection were made with 1.25g 10 wt% Nafion/DMSO solution, with 1.25 mg α -TOH added, followed with abovementioned procedure to make 1 wt% α -TOH/Nafion composite membranes with the thickness of around 12 μ m.

A Pt wire with the diameter of 100 μ m and length of 10 cm was first curved to a scroll-like shape with the curving length of 5 cm, as the active portion of Pt microelectrode. The curved portion was then highly pressed with the pressure of 8 MPa to make a flattened, curved electrode, while the other side with enough strength was used as the external connection. The Pt electrode was then sandwiched in a testing membrane and a Nafion 211 membrane, and then pressed with 0.5 MPa to fabricate the bilayer membrane for *in situ* electrochemical detection.

MEAs were prepared with Pt/C catalyst layers. First, a catalyst ink was prepared by mixing 0.5 g of the Pt / C (Pt% = 70%) catalyst and adding approximately 3 g of 5% Nafion® dispersion, and 22 mL isopropanol. The catalyst was wetted by adding a few drops of

45 water before Nafion® and methanol were added to minimize the chance of fire. The ink was stirred overnight before use. Regular MEAs were prepared by spraying successive layers of this catalyst ink directly onto a composite Nafion/ α -TOH film, with Pt loading at the anode side of $0.2 \text{ mg}\cdot\text{cm}^{-2}$, and cathode side of $0.4 \text{ mg}\cdot\text{cm}^{-2}$. Two polytetrafluoroethylene (PTFE) masks were employed on each side to maintain the active area of the MEA at $2.5 \times 2.5 \text{ cm}^2$. After the catalyst layer was applied, the MEA was pressed at 0.3 MPa for the single cell assembly.

50

Fuel Cell Operation and *in situ* Electrochemical Detection

The cell was connected to the HTS PEMFC Single Cell Test Station (Shanghai Hephas Energy Corp.) and operated at various test conditions at the temperature at 65°C . Meanwhile, a Parstat 2273 electrochemical station was employed to conduct CV and Potentiostatic measurements using a Pt microelectrode as the working electrode (WE) and an anode plate as both counter (CE) and reference electrodes (RE). The detailed information can be found in Table S3.

The following operation conditions were used for electrochemistry analysis. The scanning rate of the CV method was $20 \text{ mV}\cdot\text{s}^{-1}$, the sampling speed was $1 \text{ mV}/\text{point}$, and the scanning range was $0\text{--}1.0 \text{ V}$. The scanning speed of the LSV method was $2 \text{ mV}\cdot\text{s}^{-1}$, as for other operating conditions were the same with the CV method.

60

The electrochemical surface area (ESA) in a CV measurement was calculated as Equations as follows:

$$ESA = \frac{100 \times A_d}{c \times m \times v} \quad \text{S3)}$$

$$A_d = Q_H = \int (i - i_{DL}) \quad \text{S4)}$$

The ESA unit in Eq. S3 is $\text{m}^2\cdot\text{g}^{-1}$, where A_d was the integral area of hydrogen oxidation desorption peak in CV curve (unit as $\text{A}\cdot\text{V}$). c is the coefficient of hydrogen absorbed by platinum (value as $0.21 \text{ mC}\cdot\text{cm}^{-2}$), m is the amount of platinum at the cathode (unit as mg), and v is the scanning speed of CV method (unit as $\text{mV}\cdot\text{s}^{-1}$) [25]. The integral area for the hydrogen absorption peak is computed in Eq. S4, where i represents the measure current, and i_{DL} is the current due to the electrode double layer charging.

The LSV measurements were used to calculate the hydrogen crossover rate. The short circuit current (i_{short}) was measured under N_2/N_2 atmosphere. The measured results (i_{loss}) were the sum of hydrogen crossover current ($i_{crossover}$) and i_{short} , as defined as follow:

$$i_{loss} = i_{crossover} + i_{short} \quad \text{S5)}$$

Ex situ Electrochemical Detection

In order to understand the electrochemical signature of H_2O_2 and the inhibition ability of α -TOH to H_2O_2 in proton exchange membranes, CV scans were carried out with the Pt microelectrode in $4\text{M H}_2\text{SO}_4$ acid solution saturated with either air or H_2 . Certain amount of H_2O_2 was added to the solution before the measurements. $\text{Hg}/\text{Hg}_2\text{Cl}_2$ @ 0.242 V v.s. standard hydrogen electrode (SHE) was used as the reference electrode (25°C), Pt slice as the counter electrode, and $4\text{M H}_2\text{SO}_4$ acid solution as the electrolyte. During a CV scan, the voltage was first ramped from 0.0 to 1.4 V v.s. RHE at a scan rate of $20 \text{ mV}\cdot\text{s}^{-1}$, and then decreased from 1.4 to 0.0 V . Five cycles of scans were recorded each time, and the 4th cycle of all types of scans were presented. The detailed RHE calibration method was according to the reported method [10], and is discussed in the following context.

To investigate α -TOH poisoning effect on the cathodic catalyst, 5 mg commercial JM 20% Pt on Vulcan XC-72 was dispersed in a mixture of $50 \mu\text{L}$ 5% Nafion solution, $450 \mu\text{L}$ ethanol. A suspension was obtained under ultrasonic agitation for several hours. Then $5 \mu\text{L}$ such mixture was dropped onto a glassy carbon electrode with the diameter of 5 mm . Electrochemical measurements were performed with the conventional three-electrode system by using the modified electrode as the working electrode, a platinum wire as the counter electrode, and a standard saturated calomel electrode as the reference electrode. The supporting electrolyte was 0.1 M HClO_4 solution. The polarization curves and cyclic voltammogram were obtained through RDE with the rotating speed of 900 rpm

and the scan rate of $10 \text{ mV}\cdot\text{s}^{-1}$. Note that the current was normalized to surface area of the electrode. The electrolyte was N_2 or O_2 saturated electrolyte. $1 \text{ mg } \alpha\text{-TOH}$ was also added in the working electrode for comparison.

90

Material Characterization

The nanostructure of the hybrid membranes at each fabrication stage was determined using field emission scanning electron microscopy (FESEM, FEI NOVA NanoSEM 230, USA). The distribution of ionic clusters in hybrid membranes was observed with a transmission electron microscopy (TEM, JEM 200CX, Japan). Before TEM imaging, the membrane was stained with sodium for the clear observation of the ionic clusters by dipping into 1 M NaOH solution for 24 hours and then thoroughly rinsed in distilled water. Fourier transform infrared spectra (FT-IR) of composite membranes and $\alpha\text{-TOH}$ were obtained using a Nicolet Nexus 870 spectrometer in the range of $4000\text{--}400 \text{ cm}^{-1}$.

Discussion

For ex situ chromogenic detection within Nafion aqueous solution

The chromogenic experiments is a general characterization method in photocatalyzing degrading dyes, [11] and degrading dyes with Fenton method [12]. In either procedure, because the absorbance intensity and the concentration of rhodamine B are linearly correlated, the aqueous solution system achieving equilibrium is a basic experimental detail and essential that guaranteed the reliability of acquired data [13], or a time-dependent absorbance intensity of rhodamine B is very untrustworthy and useless.

After the ex situ chromogenic detection of the solution containing H_2SO_4 and rhodamine B, H_2SO_4 was replaced with Nafion. Noting that Fenton agent is not sensitive to alcohols, such as ethanol or isopropanol, as seen in Fig. S3b, the solvent of commercial Nafion solution was dried, and the solvent was replaced with distilled water before $0.4 \text{ g}\cdot\text{L}^{-1}$ Nafion aqueous solution was added into the sample solution.

Then aliquots of H_2O_2 were added. It was found that the decrease of absorbance intensity was not as obvious as that of H_2SO_4 /Rhodamine B solution. This is probably because Nafion is more sensitive to Fenton agents and being attacked preferentially compared with H_2SO_4 that is inert to ROS. However, with certain amount of H_2O_2 continuously dropped into the solution, precipitation occurred, as seen in Fig. S3a the picture for the comparison of Nafion/rhodamine B solution without H_2O_2 and after $73.5 \text{ }\mu\text{M}$ H_2O_2 was dropped in. The precipitation attributes to the side chain scission attack at Nafion by hydroxyl radicals. [6] And hydrophobic PTFE main chains were remained that were no longer able to be dispersed in the aqueous solution. Once the precipitation occurred, the absorbance intensity decreased dramatically, which was used as the phenomenal point, representing that Nafion molecules could not keep stable and being attacked profoundly.

With accumulative $\alpha\text{-TOH}$ added and dispersed in the solution, as seen in Fig. S3c, the precipitation point was increasingly postponed. For example, the amount of H_2O_2 for precipitation is $73.5 \text{ }\mu\text{M}$ for Nafion solution without $\alpha\text{-TOH}$, while it needs $147.0 \text{ }\mu\text{M}$ H_2O_2 for Nafion solution with $98 \text{ mg}\cdot\text{L}^{-1}$ $\alpha\text{-TOH}$ for precipitation, twice of the amount for Nafion solution. This fact demonstrated the protective effect of $\alpha\text{-TOH}$ on Nafion molecules. As a result, the attempt of using $\alpha\text{-TOH}$ as the antioxidant in PEMFCs became rational and led further investigations of fuel cell tests and subsequent electrochemical detections.

For ex situ electrochemical detection

It was found that without H_2O_2 , it was a typical H_2 oxidation process with different concentration of $\alpha\text{-TOH}$, except the inhibition of Pt-O formation at high potential (Fig. S5a). H_2 was almost constantly oxidized at the potential higher than 0.1 V . With 20 ppm H_2O_2 added in the solution, an obvious H_2O_2 oxidation current could be observed at the potential begin with around 1.0 V . However, with the increase of $\alpha\text{-TOH}$ added, the oxidation of H_2O_2 was increasingly inhibited (Fig. S5b), probably caused by $\alpha\text{-TOH}$ reduction of

H₂O₂. Similar phenomena were also found in saturated O₂ environment. Without H₂O₂, the CV scans were typical oxygen reduction reactions; while more added α -TOH only led to the inhibition of limiting current (Fig. S5c). With 20 ppm H₂O₂ added, the H₂O₂ oxidation current was also observed with the potential higher than 1.0 V. And the increase of added α -TOH also led to the inhibition of H₂O₂ oxidation current (Fig. S5d). After the initial CV scan under O₂ environment, solution with 100 mg·L⁻¹ α -TOH and 20 ppm H₂O₂ was again settled in the saturated H₂ environment for further observation. Interestingly, it was found the increase of H₂ oxidation current in the period of 2 hours (Fig. S5e). After that, with the change of environment from H₂ to O₂, obvious depression of H₂O₂ signature was found (Fig. S5d), indicating that electrons from H₂ was firstly donated to drive α -TOH reduction instead of being drawn to the Pt microelectrode, leading to refunctionalization of α -TOH as a reductant.

140

For long-range OCV holding test

For OCV holding test, the hydrogen crossover current density, also nominated as hydrogen crossover rate (HCR), was measured with Linear scanning voltammetry (LSV) from 0.10 – 0.45 V under the H₂/N₂ circumstance at 65 °C. For the purpose of better comparison during OCV holding test, the current density at a voltage = 0.3 V was collected. For each voltage and power density point in the polarization curve, a 3 min galvanostatic process was used with a record rate of 1 point/sec, followed with the next current density to acquire a full scale of polarization curve. 180 points of voltage and power density value with certain current density was averaged. And this process was repeated for 8 times. The final values and errors were averaged and calculated from the 8 single polarization curves.

150 Over time the chemical attack leads to membrane degradation and thinning, both facilitating reactant gas crossover, which in turn facilitates the formation of hydrogen peroxide [7]. As a result, hydrogen crossover rate is one of the key parameter to evaluate the chemical stability of proton exchange membranes. For long-range chemical stability of PEM during operation, with similar initial membrane thicknesses, it was observed that after 5 cycles, hydrogen crossover rate of MEA with recasted Nafion can be as high as 2.6 mA·cm⁻² (Fig. 8e). However, it needed 11 cycles for Nafion/1.5% α -TOH to reach this level. (Fig. S6) This fact can be treated as one of the major proof of the chemical stability of PEM with the protection of α -TOH.

Further, OCV holding tests for Nafion/1.5% α -TOH lasted for 15 cycles, as seen in Fig. S6, until the hydrogen crossover rate reached the value around ~10 mA·cm⁻². Within these 15 cycles, the voltage at mass-transfer region of polarization curve kept at a high level, even after 15 OCV holding cycles, which is another proof of the chemical stability of the composite membrane.

160

For influence of α -TOH on the durability of PEMs

In order to check out the catalyst activity, the potential changes as the function of logarithmic current density were compared to have a closer look to the activation-loss regions of Fig 3a – d, as shown as Fig. S6. It was observed that after OCV holding test and recovery test, the activation-loss region of MEA with solution-cast Nafion exhibited obvious and unrecoverable depress, indicating a obvious kinetic loss, which were probably caused by the poor three-phase contact. However, the kinetic region of MEAs with all composite membranes showed minor change after OCV holding tests and the recovery process, indicating much less kinetic loss in the MEAs of composite membranes. Especially for MEA with Nafion/3% α -TOH composite membrane, only ignorable change could be observed, compared with that of solution-cast Nafion, indicating the protective function of α -TOH to the fuel cells.

170 Furthermore, the activation-loss region of MEA of both Nafion/1.5% α -TOH composite membrane and recasted Nafion membrane was also carefully examined, as illustrated in Fig. S7. It was found that MEA with Nafion membrane shows a minor change during 5-cycle OCV holding tests. For the Nafion/1.5% α -TOH composite membrane, a slight drop of voltage was observed after 2 cycles, however it followed by a dramatic increase at the next cycle, which was even higher than the initial value. It was believed that this temporary drop was not caused by the bad three-phase contact between the catalyst and the electron/proton conductor that leads to the activity loss of catalyst, since such performance loss at the activation-region was mainly caused by Pt drain [8], and carbon degradation [9], which is generally unrecoverable.

It was believed that the leakage of α -TOH onto the cathode can hinder the fuel cell performance, causing cathodic catalyst poisoning. This fact can be used to explain the sudden drop and recovery of voltage at both the activation-loss and the mass-transfer region during OCV holding tests and polarization curve measurements. As a result, a simulating experiment was designed and made.

The comparison of cathodic catalysts with or without α -TOH was shown in Fig. S8. It was interesting that other than redox reactions of α -TOH that could be hardly found on bulk Pt wire as the working electrode (see Fig. S4c and S4d), the redox peaks of α -TOH was strongly magnified with nanosized Pt/C catalyst, probably because of the nano-size effects of Pt and their better contact with α -TOH, as seen in Fig. S8b. After the α -TOH addition, both redox peaks of α -TOH were found with N_2 and O_2 saturated electrolytes. Especially in N_2 saturated electrolyte, two separated peaks at around 0.43 and 0.54 V were observed, indicating two separated one-electron reaction of α -TOH oxidation and reduction (see Eq. 3 – 8), compared with the combined redox peak at 0.45 V for oxidation and 0.37 V for reduction in the O_2 saturated electrolyte. It was possible that under O_2 saturated atmosphere, the redox reaction was accelerated because of the abundance of oxidants, leading to the combined redox peaks instead of distinct peaks shown in N_2 atmosphere. As a result, the ORR polarization curve of Pt/C with α -TOH fluctuated as seen in Fig. S8c.

Furthermore, an obviously higher voltage drop can be observed for ORR catalysts added with α -TOH, compared with pristine Pt/C catalyst at both the activation-loss and the mass-transfer regions, indicating the poisoning effects of α -TOH on ORR catalyst. Comparison of CV scans under N_2 atmosphere (Fig. S8d) also showed the inhibited hydrogen oxidation desorption capability caused by α -TOH addition.

Conclusively, it is rational to postulate that during fuel cell performance test, part of α -TOH leaks to the cathode side, poisoning the ORR catalysts, leading to a performance loss during polarization curve measurements. After the next cycle of 24 hr OCV holding tests, since the leaked α -TOH is consumptively oxidized at the high potential level. The performance is then recovered.

After 5-cycle OCV holding tests, the SEM images of cross-sectional view of membranes for both solution-cast Nafion and Nafion/1.5% α -TOH composite membranes were compared, as shown in Fig. S9. It could be observed that after 5-cycle OCV holding test, the thickness of solution-cast Nafion decreased from 40 μm to around 15 μm , indicating severe membrane thinning during fuel cell operation. However, Nafion/1.5% α -TOH composite membranes remained at the thickness around 40 μm , while the α -TOH nano-droplets (Fig. S9b, d) seemed invisible, indicating the preferential oxidative consumption of α -TOH, and much reduced membrane degradation due to the additive of α -TOH.

RHE calibration

During in situ H_2O_2 detection, since the anode side is $H_2/Pt/H^+$ interfaces, as a result, the reference electrode was directly connected to the anode, the data were easy to acquire and calculate. During *ex situ* H_2O_2 detection, it is quite difficult to make sure the activity ($a[H^+]$) value for 4 M H_2SO_4 solution. As a result, we used saturated calomel electrode (SCE) as the reference electrode in all measurements. It was calibrated with respect to reversible hydrogen electrode (RHE) according to the reported method[10]. The calibration was performed in the high purity hydrogen saturated electrolyte with a Pt wire as the working electrode. CV were run at a scan rate of 1 mV s^{-1} , and the average of the two potentials at which the current crossed zero was taken to be the thermodynamic potential for the hydrogen electrode reactions. As seen in figure S8. It was measured the $E(0)$ was -0.211 V. So in 4 M H_2SO_4 , $E(RHE) = E(SCE) + 0.211 V$.

Figure:

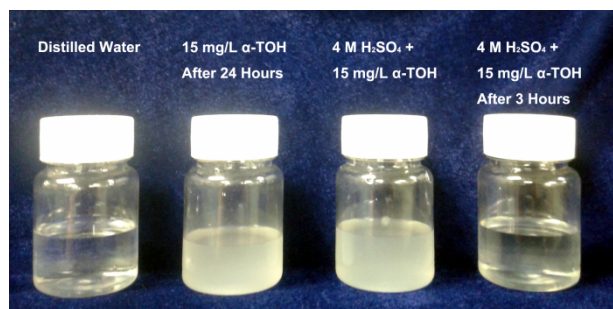


Figure S1. Comparison of α -TOH dispersity in different solutions. It could be observed that $15 \text{ mg} \cdot \text{L}^{-1}$ α -TOH can be uniformly dispersed in distilled water to make a milky dispersion, such dispersion could be stable even after 24 hours without obvious change. However, in H_2SO_4 solution, α -TOH could be better dispersed. For example, $4 \text{ M H}_2\text{SO}_4$ dispersed with $15 \text{ mg} \cdot \text{L}^{-1}$ α -TOH could change limpid in less than 3 hours.

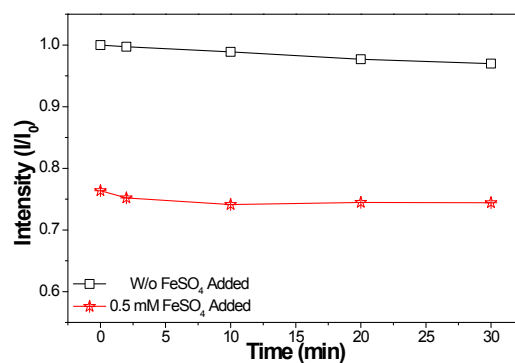
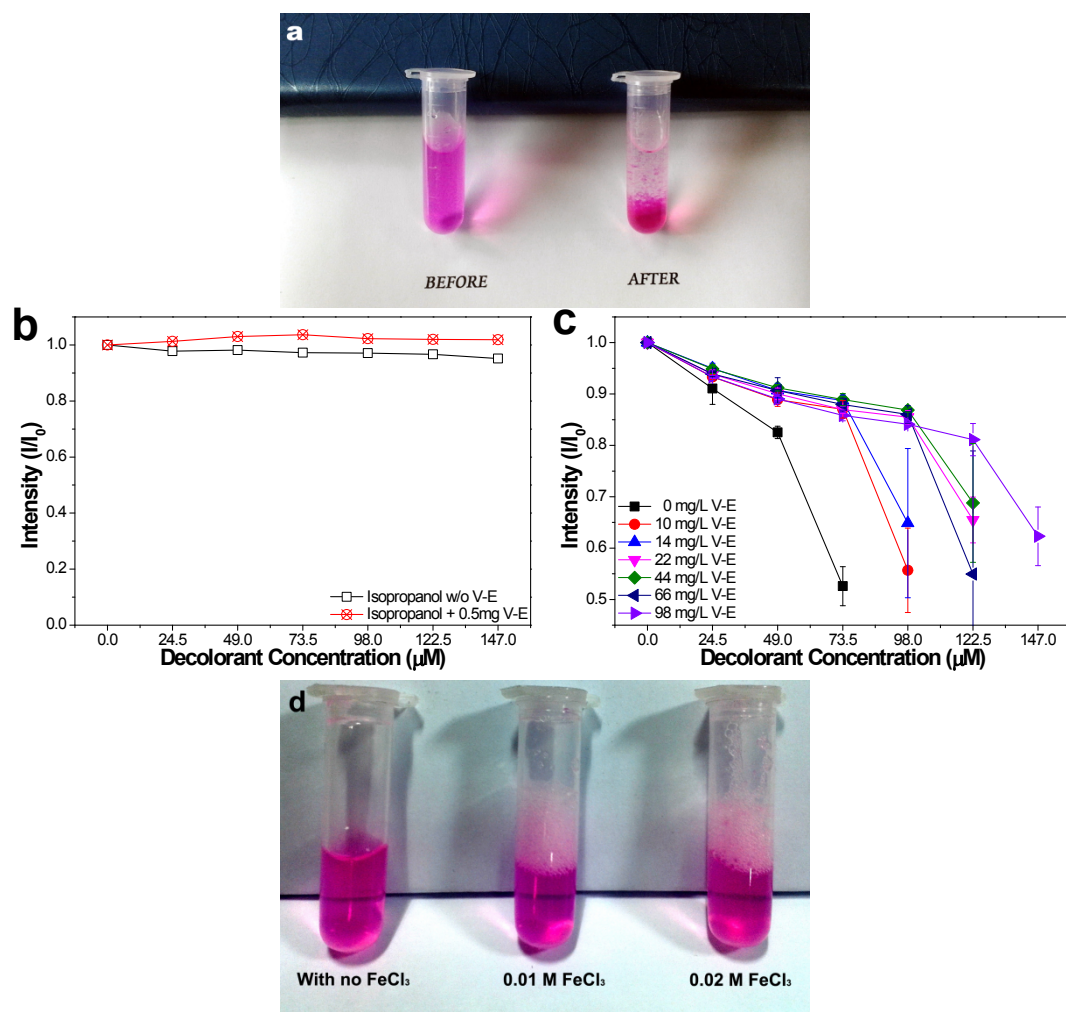


Figure S2. Stability of rhodamine B in H₂SO₄ solution. The solution of 1M H₂SO₄, 2mg·L⁻¹ α-TOH, 24.5 μM H₂O₂ and 12.5μM rhodamine B was observed. Before the Fe²⁺ catalyst was added, the absorbance of the solution at 550 nm was almost kept as a constant; while as soon as the catalyst was added, the color fading was observed. And such color intensity could keep constantly in as long as 30 min, and without change of absorbance thereafter.



235 **Figure S3. chromogenic experiment for Nafion solution.** **a.** The aqueous solution of $0.4 \text{ g}\cdot\text{L}^{-1}$ Nafion, 0.5 mM FeSO_4 , $12.5 \text{ }\mu\text{M}$ rhodamine B before H_2O_2 was added and after $73.5 \text{ }\mu\text{M}$ H_2O_2 added. Before H_2O_2 addition, the solution kept stable; while with H_2O_2 added, the precipitation occurred soon after. **b.** The inhibition of isopropanol to fenton agents. **c.** The influence of α -TOH on the precipitation of Nafion as the function of the concentration of H_2O_2 . The sharp drop of absorbance intensity is caused by the precipitation of Nafion, used as phenomenal point that Nafion molecules could not keep stable and being attacked profoundly. It was observed that for $0.4 \text{ g}\cdot\text{L}^{-1}$ Nafion solution, this point is $73.5 \text{ }\mu\text{M}$ H_2O_2 for Nafion solution without α -TOH, $98.0 \text{ }\mu\text{M}$ for 10 and $14 \text{ mg}\cdot\text{L}^{-1}$ α -TOH, $122.5 \text{ }\mu\text{M}$ for 22 , 44 , and $66 \text{ mg}\cdot\text{L}^{-1}$ α -TOH, and $147.0 \text{ }\mu\text{M}$ H_2O_2 for $98 \text{ mg}\cdot\text{L}^{-1}$ α -TOH. **d.** $0.25 \text{ wt}\%$ Nafion aqueous solution added with aliquots of FeCl_3 , to make sure the possible influence of ionic crosslinking of Nafion caused by Fe^{3+} . It can be observed that with 0.02 M FeCl_3 in the solution, no obvious precipitate occurred. However, it seemed that the solution became more viscous somehow, indicating there might be ionic crosslinking of Nafion molecules with FeCl_3 . However, this is not the reason of the precipitation occurring during Fenton reactions.

240

245

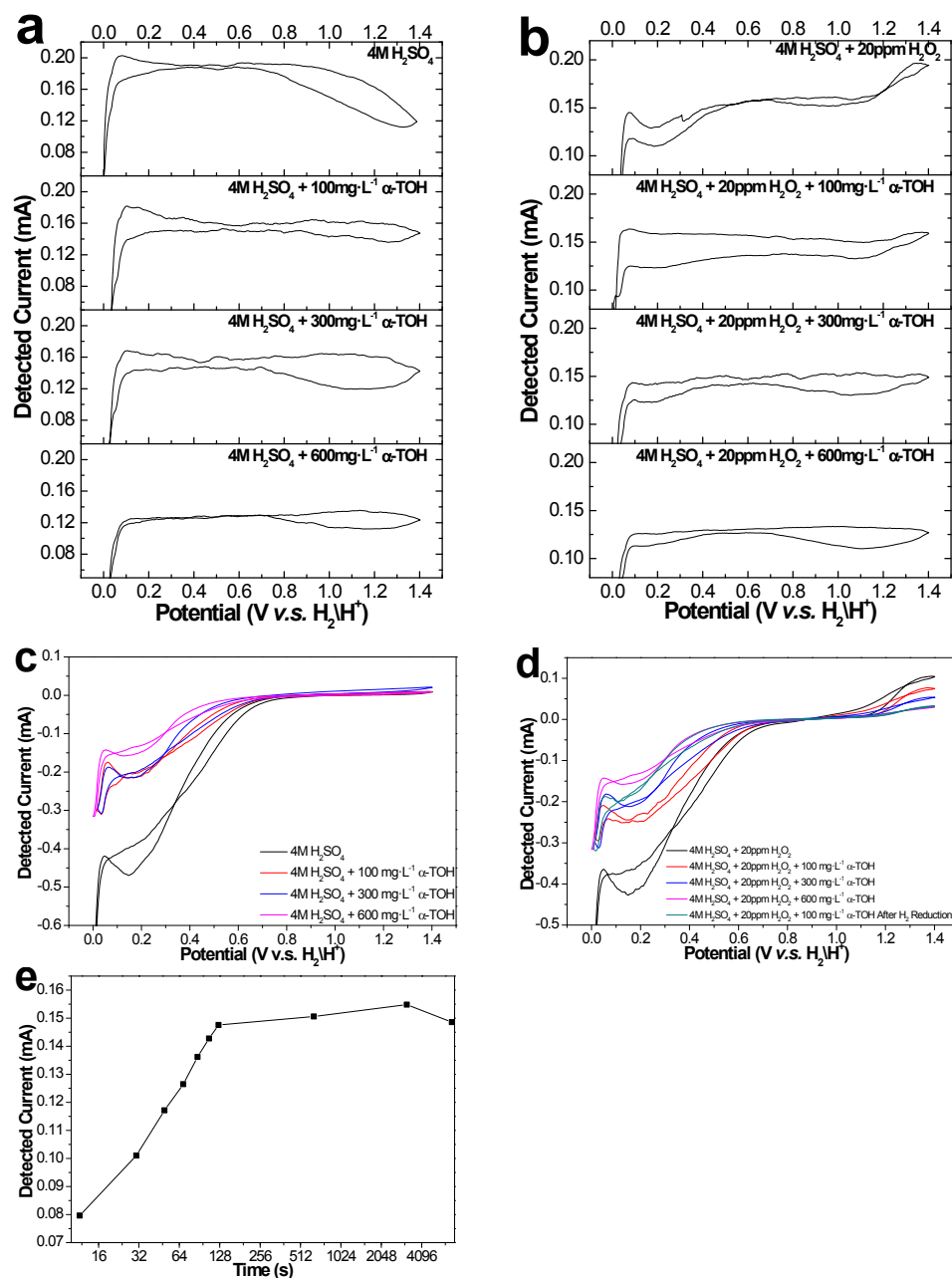


Figure S4. Ex situ electrochemical detection of α -TOH in acidic solution. **a.** CV scans in 4 M H_2SO_4 with different amount of α -TOH in saturated H_2 environment. **b.** CV scans in 4 M H_2SO_4 , 20 ppm H_2O_2 with different amount of α -TOH in saturated H_2 environment. **c.** CV scans in 4 M H_2SO_4 with different amount of α -TOH in saturated O_2 environment. **d.** CV scans in 4 M H_2SO_4 , 20 ppm H_2O_2 with different amount of α -TOH in saturated O_2 environment. **e.** Hydrogen oxidation current at 0.3 V during the period of H_2 reduction process.

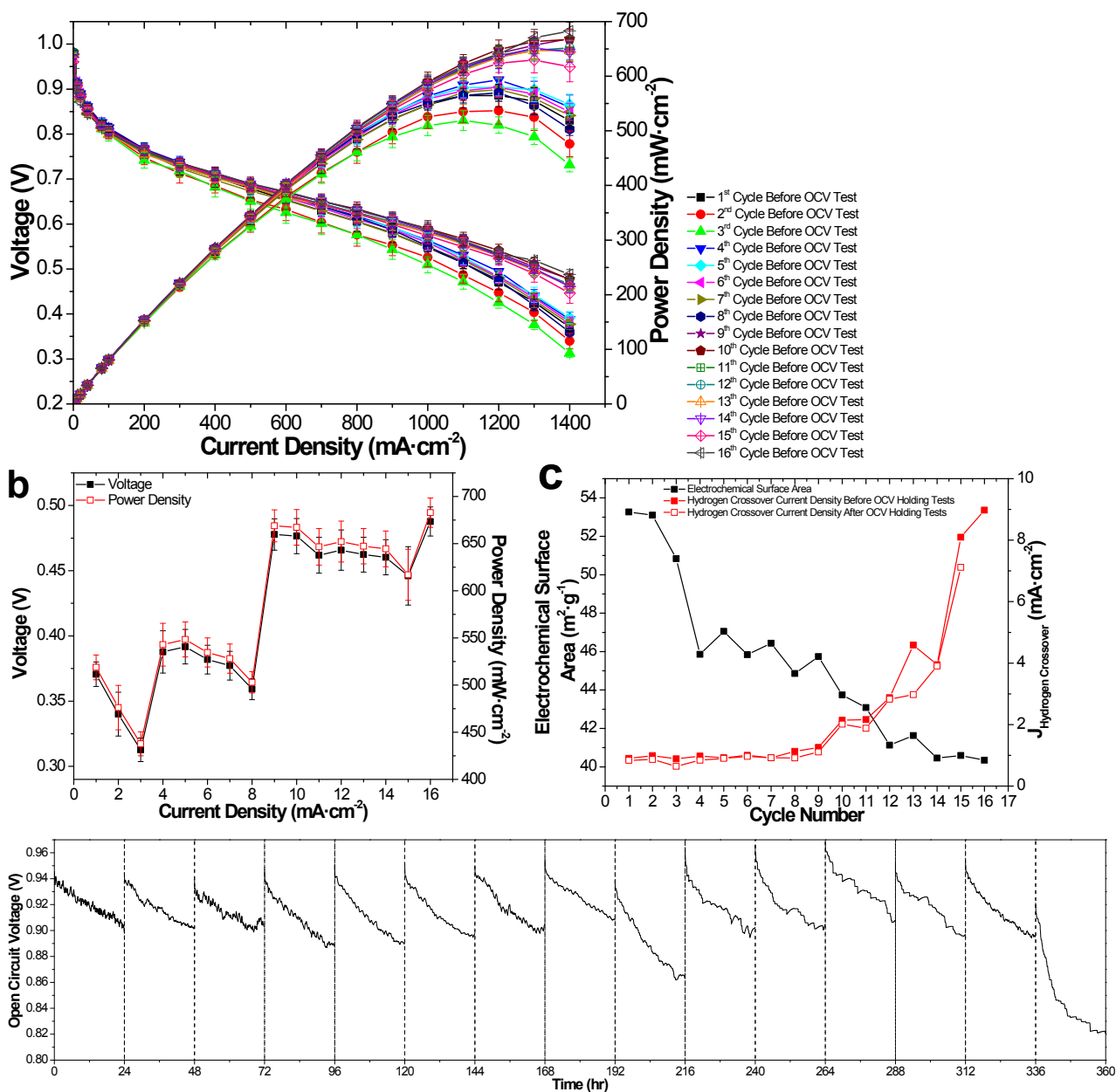
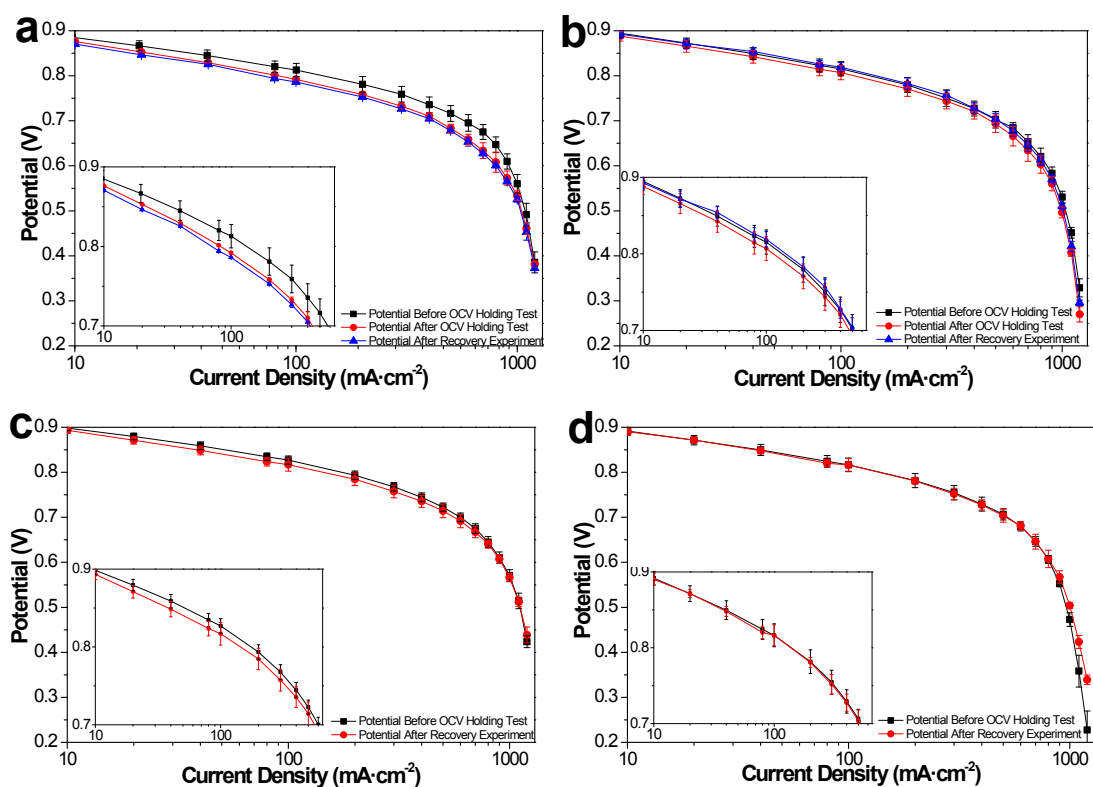


Figure S5. Long-range OCV holding test for MEA with Nafion/1.5% α -TOH composite membrane. a. Polarization curves and power output of PEM single fuel cells for 15 cycles. **b.** The variation of potential at $1400 \text{ mA}\cdot\text{cm}^{-2}$ (peak of power output) after each OCV holding tests. **c.** The variation of Electrochemical surface area and hydrogen crossover current density. Specifically, the hydrogen crossover current densities at different timeline were compared, indicating the reduction of hydrogen crossover rate after OCV holding tests. **d.** OCV drop with the increase of cycle number were also shown.



5 **Figure S6. Variation of fuel cell performance before and after OCV holding tests.** Polarization curves of PEM single fuel cells with **a.** recasted Nafion, **b.** Nafion/0.5% α -TOH, **c.** Nafion/1% α -TOH, and **d.** Nafion/3% α -TOH composite membrane. Potential v.s. logarithmic current density were shown for better comparison of kinetic regions of fuel cell performance before, after OCV holding tests and after recovery experiment. Comparison of performance between recasted Nafion and Nafion/0.5% α -TOH composite membrane after recovery procedure were shown in **a.** and **b.** respectively. And the insets were enlarged view on the current density from 10 to 650 $\text{mA}\cdot\text{cm}^{-2}$.

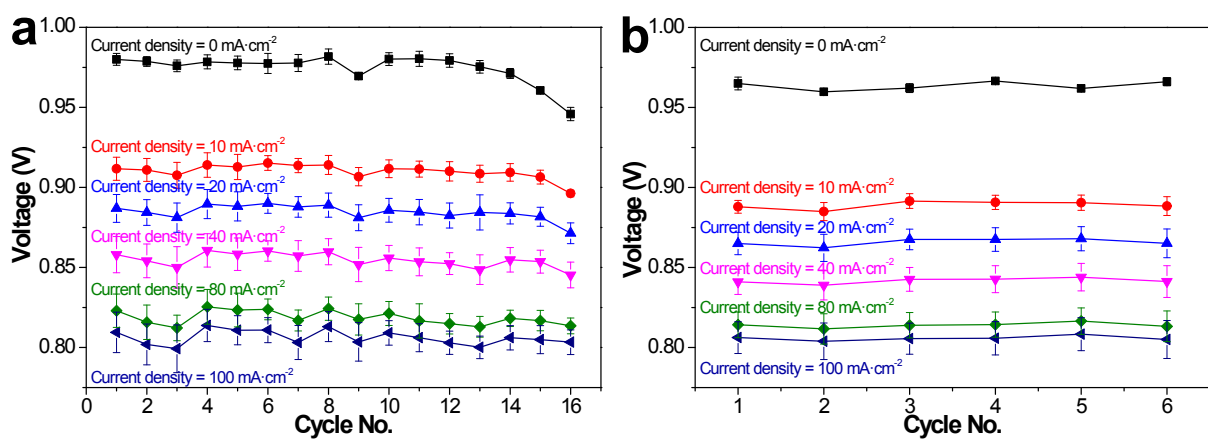


Figure S7. The change of single cell voltage at activation-loss region as the function of the OCV holding test cycle number with certain current density of a) Nafion/1.5% α -TOH composite membrane, and b) recasted Nafion membrane. The cell voltage from OCV(current density = 0) to ~ 0.8 V (current density = 100 mA·cm⁻²) was compared respectively.

5

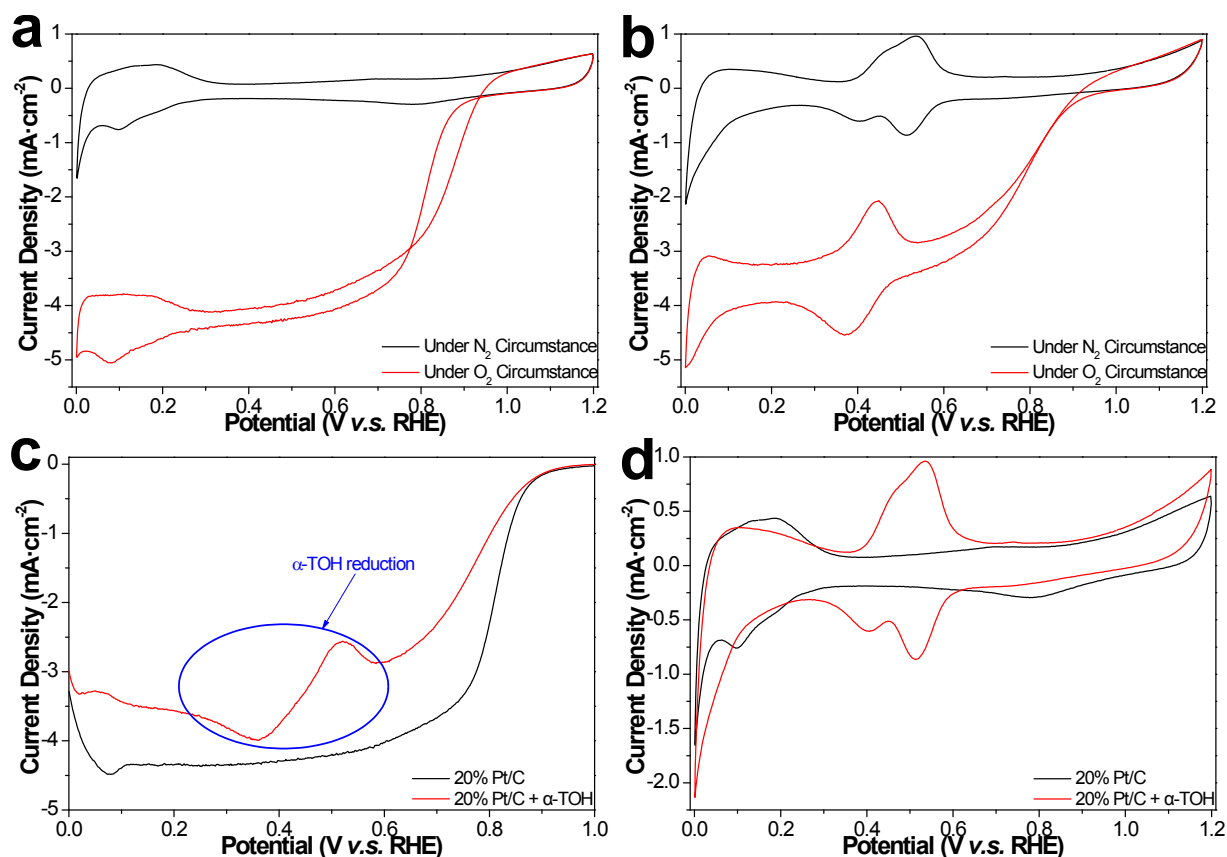


Figure S8. Electrochemical measurements of glassy carbon electrode coated with 20% Pt/C catalyst with or without 1 mg α-TOH. Cyclic voltammogram of Pt/C catalyst **a.** without and **b.** with 1 mg α-TOH under saturated O₂/N₂ atmospheres. **c.** Comparison of polarization curves of oxygen reduction reactions on the catalysts with or without α-TOH. The fluctuation for Pt/C with α-TOH is caused by α-TOH reduction. **d.** Cyclic voltammogram of both Pt/C catalysts with or without α-TOH under N₂ atmosphere was also compared, indication inhibited hydrogen oxidation desorption capability on α-TOH stained catalysts.

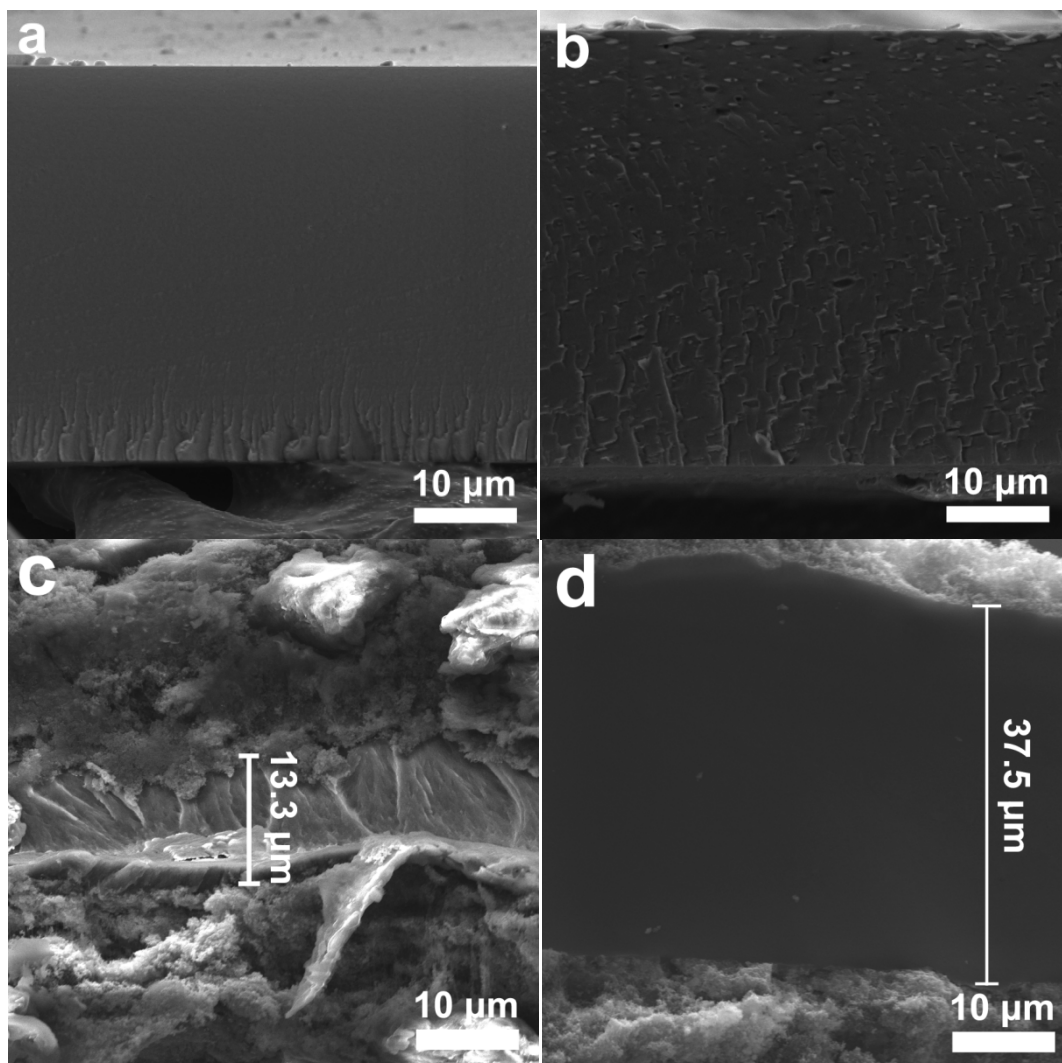


Figure S9. Comparison of SEM images of cross-section view on the membranes before and after 5-cycle OCV tests. **a)** solution-cast Nafion membrane, and **b)** Nafion/1.5% α -TOH composite membrane with the average thickness of around 40 μm before OCV holding tests; **c)** CCM of solution-cast Nafion with the average thickness of around 15 μm , **d)** CCM of Nafion/1.5% α -TOH composite membrane with the average thickness of around 40 μm .

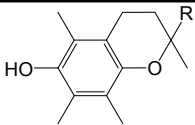
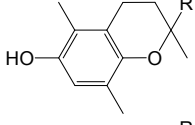
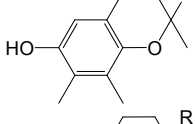
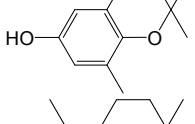
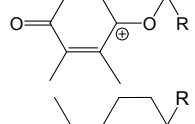
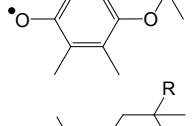
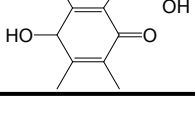
Table S1. Overview of reactions involving intermediates considered in this study that describe the generation and consumption of ROS by ionomer Nafion, and free radical scavenger

#	Reactions	References
<i>Free Radical Generation</i>		
1	$H_2 + Pt \rightarrow Pt - H \text{ (at anode)}$	2
2	$Pt - H + O_2 \text{ (diffused through PEM to anode)} \rightarrow HOO^\cdot$	2
3	$HOO^\cdot + Pt - H \rightarrow H_2O_2$	2
4	$H_2O_2 \rightarrow 2HO^\cdot$	3
5	$HO^\cdot + H_2O_2 \rightarrow HOO^\cdot + H_2O$	3
6	$HO^\cdot + H_2 \rightarrow H^\cdot + H_2O$	3
7	$H^\cdot + O_2 \rightarrow HOO^\cdot$	3
8	$HOO^\cdot + H_2O_2 \rightarrow HO^\cdot + H_2O + O_2$	3
9	$2HOO^\cdot \rightarrow H_2O_2 + O_2$	3
10	$Fe^{2+} + H_2O_2 + H^+ \rightarrow Fe^{3+} + HO^\cdot + H_2O$	3
11	$Fe^{2+} + HO^\cdot + H^+ \rightarrow Fe^{3+} + H_2O$	3
12	$Fe^{2+} + HOO^\cdot + H^+ \rightarrow Fe^{3+} + H_2O_2$	3
13	$Fe^{3+} + HOO^\cdot \rightarrow Fe^{2+} + O_2 + H^+$	3
14	$Fe^{3+} + H_2O_2 \rightarrow Fe^{2+} + HOO^\cdot + H^+$	3
<i>Ionomer Chemical Degradation</i>		
15	$R_f - CF_2COOH + HO^\cdot \rightarrow R_f - CF_2^\cdot + CO_2 + H_2O$	2
16	$R_f - CF_2^\cdot + HO^\cdot \rightarrow R_f - CF_2OH + R_f - COF + HF$	2
17	$R_f - COF + H_2O \rightarrow R_f - COOH + HF$	2
<i>α-TOH Protection of PEM</i>		
18 ^a	$HOO^\cdot + \alpha - TOH \rightarrow H_2O_2 + \alpha - TO^\cdot$	4
19 ^a	$HOO^\cdot + \alpha - TO^\cdot \rightarrow (\alpha - TO)OOH$	4
20 ^a	$OH^\cdot + \alpha - TOH \rightarrow H_2O + \alpha - TO^\cdot$	14
21 ^a	$OH^\cdot + \alpha - TO^\cdot \rightarrow (\alpha - TO)OH$	14
22	$2\alpha - TO^\cdot + H_2 \rightarrow 2\alpha - TOH$	14
23	$\alpha - TO^+ + H_2 \rightarrow \alpha - TOH + H^+$	14
<i>α-TOH side reactions^b</i>		
24	$\alpha - TO^\cdot + H^+ \rightarrow \alpha - TOH^{\cdot+}$	4
25	$\alpha - TO^+ + H^+ \rightarrow \alpha - TOH^{2+}$	4
26	$TOH + O^\cdot \rightarrow (TOH)O$	14
27	$TO^\cdot + TO^\cdot \rightarrow TO - TO$	14

^a. Detailed illustration could be found in Scheme S1.

^b. The side reactions listed is not limited in these 4 reactions.[14]

Table S2 Chemical formula of major reactors and products^a

material	Short Form	Formula
α -tocopherol	α -TOH	
β -tocopherol	β -TOH	
γ -tocopherol	γ -TOH	
δ -tocopherol	δ -TOH	
α -tocophenoxonium cation	α -TO ⁺	
α -tocopheroxy radical	α -TO [•]	
α -tocopherolquinine	(α -TO)O	

^a R = (CH₂CH₂CH₂CH(CH₃))₃CH₃

Table S3 Testing Condition of Single Cell Measurement^a

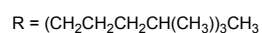
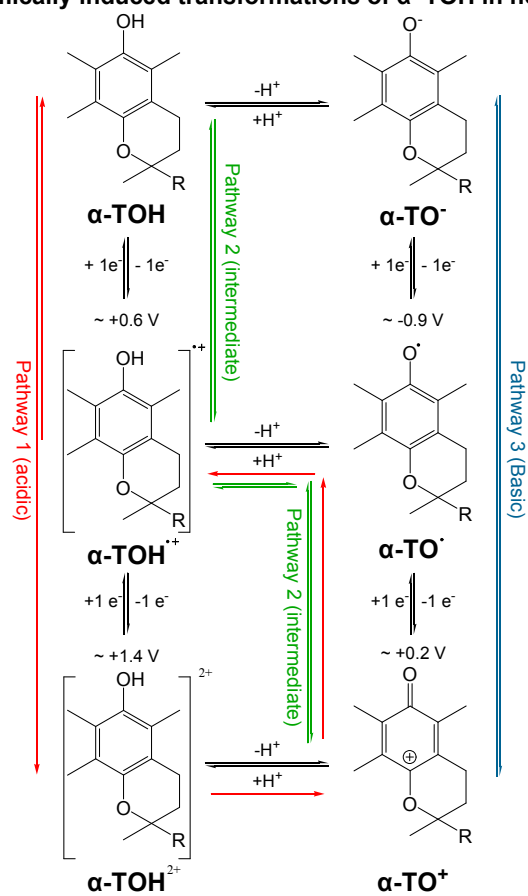
Measurements	Temperature (°C)	Atmosphere	Gas Pressure (Pa)	Gas Flow Rate (sccm)	Relative Humidity (%)
Polarization Curve Measurement	65	H ₂ /air	1.01 × 10 ⁵	A:200 + 2 stoi. × i ^b C:500 + 3 stoi. × i	100%
OCV Holding Test	65	H ₂ /air	1.01 × 10 ⁵	A:200 C:500	30%
Cyclic Voltammetry	65	H ₂ /N ₂	1.01 × 10 ⁵	A:200 C:200	100%
Linear Sweep Voltammetry	65	H ₂ /N ₂	1.01 × 10 ⁵	A:200 C:200	100%

^a: Area = 2.5 × 2.5 cm²,

^b: A = Anode, C = Cathode;

^c: i = current of single cell.

Scheme S1 Electrochemically induced transformations of α -TOH in non-aqueous solvent ^{a, 4, 5}



a. Listed potentials were voltammetric potentials v.s. Fc/Fc⁺

Reference:

- [1] S. Akyuza, J. E. D. Davies, Temperature dependent FTIR spectroscopic study of the interaction of α -tocopherol and α -tocopheryl acetate with phospholipid bilayers, *J. Mol. Struct.* **1997**, *415*, 65 – 70.
- 5 [2] R. Borup, J. Meyers, B. Pivovar, Y. S. Kim, R. Mukundan, N. Garland, D. Myers, M. Wilson, F. Garzon, D. Wood, P. Zelenay, K. More, K. Stroh, T. Zawodzinski, J. Boncella, J. E. McGrath, M. Inaba, K. Miyatake, M. Hori, K. Ota, Z. Ogumi, S. Miyata, A. Nishikata, Z. Siroma, Y. Uchimoto, K. Yasuda, K. Kimijima, N. Iwashita, Scientific Aspects of Polymer Electrolyte Fuel Cell Durability and Degradation, *Chem. Rev.* **2007**, *107*, 3904 – 3951.
- [3] L. Gubler, S. M. Dockheer, W. H. Koppenol, Radical (HO^\bullet , H^\bullet and HOO^\bullet) Formation and Ionomer Degradation in Polymer Electrolyte Fuel Cells. *J. Electrochem. Soc.* **2011**, *158*, B755 – B769.
- 10 [4] R. D. Webster, New Insights into the Oxidative Electrochemistry of Vitamin E. *Acc. Chem. Res.* **2007**, *40*, 251 – 257.
- [5] L. L. Williams, R. D. Webster, Electrochemically Controlled Chemically Reversible Transformation of α -Tocopherol (Vitamin E) into Its Phenoxonium Cation, *J. Am. Chem. Soc.* **2004**, *126*, 12441 – 12450.
- [6] L. Ghassemzadeh, K.D. Kreuer, J. Maier, K. Müller, *J. Power Sources*, **2011**, *196*, 2490 – 2497.
- [7] W. Schmittinger, A. Vahidi, *J Power Sources*, **2008**, *180*, 1 – 14.
- 15 [8] P. J. Ferreira, G. J. la O', Y. Shao-Horn, D. Morgan, R. Makharia, S. Kocha, H. A. Gasteiger, *J. Electrochem. Soc.* **2005**, *152*, A2256-A2271.
- [9] J.-H. Park, S.-D. Yim, T. Kim, S.-H. Park, Y.-G. Yoon, G.-G. Park, T.-H. Yang, E.-D. Park, *Electrochim. Acta*, **2012**, *83*, 294–304.
- [10] Y. Liang, Y. Li, H. Wang, J. Zhou, J. Wang, T. Regier, H. Dai, *Nat. Mater.* **2011**, *10*, 780 – 786.
- 20 [11] Y. Huang, Z. Zheng, Z. Ai, L. Zhang, X. Fan, Z. Zou, *J. Phys. Chem. B*, **2006**, *110*, 19323–19328.
- [12] Z. Ai, L. Lu, J. Li, L. Zhang, J.g Qiu, M. Wu, *J. Phys. Chem. C*, **2007**, *111*, 4087 – 4093.
- [13] V. Prabhakaran, C. G. Arges, V. Ramani, *PNAS*, **2012**, *109*, 1029 – 1034.
- [14] Afaf Kamal-Eldin, L.-A. Appelqvist, *Lipids*, **1996**, *37*, 671 – 701